Meteoritics & Planetary Science 38, Nr 10, 1499–1506 (2003)
Abstract available online at http://meteoritics.org

Northwest Africa 428: Impact-induced annealing of an L6 chondrite breccia

Alan E. RUBIN

Institute of Geophysics and Planetary Physics, University of California, Los Angeles, California 90095–1567, USA
E-mail: aerubin@ucla.edu

(Received 23 May 2003; revision accepted 17 October 2003)

Abstract–Northwest Africa (NWA) 428 is an L chondrite that was successively thermally metamorphosed to petrologic type-6, shocked to stage S4–S5, brecciated, and annealed to approximately petrologic type-4. Its thermal and shock history resembles that of the previously studied LL6 chondrite, Miller Range (MIL) 99301, which formed on a different asteroid. The petrologic type-6 classification of NWA 428 is based on its highly recrystallized texture, coarse metal (150 ± 150 μm), troilite (100 ± 170 μm), and plagioclase (20–60 μm) grains, and relatively homogeneous olivine ($Fa_{24.4 \pm 0.6}$), low-Ca pyroxene ($Fs_{20.5 \pm 0.4}$), and plagioclase ($Ab_{84.2 \pm 0.4}$) compositions. The petrographic criteria that indicate shock stage S4–S5 include the presence of chromite veinlets, chromite-plagioclase assemblages, numerous occurrences of metallic Cu, irregular troilite grains within metallic Fe-Ni, polycrystalline troilite, duplex plessite, metal and troilite veins, large troilite nodules, and low-Ca clinopyroxene with polysynthetic twins. If the rock had been shocked before thermal metamorphism, low-Ca clinopyroxene produced by the shock event would have transformed into orthopyroxene. Post-shock brecciation is indicated by the presence of recrystallized clasts and highly shocked clasts that form sharp boundaries with the host. Post-shock annealing is indicated by the sharp optical extinction of the olivine grains; during annealing, the damaged olivine crystal lattices healed. If temperatures exceeded those approximating petrologic type-4 (~600–700°C) during annealing, the low-Ca clinopyroxene would have transformed into orthopyroxene. The other shock indicators, likewise, survived the mild annealing. An impact event is the most plausible source of post-metamorphic, post-shock annealing because any ^{26}Al that may have been present when the asteroid accreted would have decayed away by the time NWA 428 was annealed. The similar inferred histories of NWA 428 (L6) and MIL 99301 (LL6) indicate that impact heating affected more than 1 ordinary chondrite parent body.

INTRODUCTION

Although numerous researchers have advocated the decay of ^{26}Al to ^{26}Mg ($t_{½}$ = 0.72 Ma) as the principal mechanism of asteroidal heating (e.g., Urey 1955; Reeves and Audouze 1968; Herndon and Herndon 1977; Grimm and McSween 1989, 1993; Akridge et al. 1998; Wilson et al. 1999; Keil 2000; McSween et al. 2002), increasing evidence exists that members of different chondrite groups experienced a complicated history of thermal metamorphism, shock metamorphism, and post-shock annealing. These late-stage annealing events seem to have resulted from impact heating.

Some EL6 chondrites are brecciated (e.g., Hvittis and Atlanta; Rubin 1983a, b) and others appear to be impact-melts (e.g., Blithfield; Rubin 1984), implying that these rocks were once appreciably shocked. Nevertheless, on the basis of the undulose extinction of their orthopyroxene (and absence of clinoenstatite lamellae and mosaicism), these rocks are classified as shock stage S2 (very weakly shocked). It seems probable that these EL6 chondrites were shocked and annealed (Rubin et al. 1997). (They may have been annealed to stage S1 and then shocked again to reach stage S2.)

The Elephant Moraine (EET) 87507 CK5 chondrite and its paired specimens exhibit major silicate darkening and contain 3–5 mm-long shock veins containing small pentlandite and magnetite grains (Rubin 1992). Although classified as shock stage S2, this rock is likely to have reached stage S4–S5 and then been annealed. (It also may have been annealed to stage S1 and shocked again to reach stage S2.)

Rubin (Forthcoming) examined 53 type-5 and -6 ordinary chondrites (OC) of shock stage S1 (38 H, 11 L, 4 LL) and found that every one possessed 2 or more relict shock indicators, implying that these rocks experienced post-shock annealing. The shock indicators include chromite veinlets, chromite-plagioclase assemblages, metal and sulfide veins, polycrystalline troilite, rapidly solidified metal-sulfide

intergrowths, metallic Cu, large troilite nodules, silicate-rich melt pockets, and devitrified silicate-rich melt veins. In the case of the MIL 99301 LL6 chondrite (Rubin 2002), the Ar-Ar age spectrum indicates that post-shock annealing took place ~4.26 Ga ago (Dixon et al. 2003), long after any ^{26}Al that may have been present when the asteroid accreted had decayed away.

Although derived from a different parent asteroid than MIL 99301 (LL6), the L6 chondrite Northwest Africa (NWA) 428, seems to have experienced a similar thermal and shock history, as indicated by incomplete annealing of shock effects. It was purchased by Western dealers in Morocco in 2001 as a single 655 g mass; whether it was collected in Morocco, Algeria or the Western Sahara is unknown (Russell et al. 2003).

ANALYTICAL PROCEDURES

A ~4 cm-long slab of NWA 428 (LC 1887) in the UCLA meteorite collection was examined macroscopically. Thin sections UCLA 1462 and 1682 were studied microscopically in transmitted and reflected light. Mineral analyses were made with the JEOL JXA-8200 electron microprobe at UCLA using natural and synthetic standards, an accelerating voltage of 15 keV, a 15 nA sample current, 20 sec counting times, and ZAF corrections.

RESULTS AND DISCUSSION

Weathering Grade

NWA 428 exhibits evidence of only slight weathering, corresponding to weathering stage W1 (Wlotzka 1993). Silicates exhibit moderate brown staining. Most metallic Fe-Ni grains are free of limonite; although, some have thin (~1–2 μm-wide) limonite rinds. Rare metal grains, particularly those near the meteorite surface, have thicker rinds. Most troilite grains are completely free of terrestrial alteration products; however, a few 10–30 μm-thick limonite veins transect one of the large troilite nodules.

Chondrite Group

The mean compositions of olivine and low-Ca pyroxene in NWA 428 (Table 1) are $Fa_{24.4}$ mol% and $Fs_{20.5}Wo_{1.7}$ mol%, respectively, in the middle of the L chondrite ranges ($Fa_{23.0–25.8}$ mol%, $Fs_{18.7–22.6}$ mol%; Rubin 1990; Gomes and Keil 1980). The mean plagioclase composition ($Ab_{84.2}Or_{5.5}$ mol%; Table 1) is essentially identical to that of mean L chondrites ($Ab_{84.2}Or_{5.6}$ mol%; Van Schmus and Ribbe 1968). The mean chromite composition (Table 1) is within the L chondrite ranges for all of the major oxides (Fig. 191 in Brearley and Jones [1998]). The modal abundance of metallic Fe-Ni is 7.3 wt% (Table 2), near the center of the range of L chondrite falls (5.3–10.4 wt%; Jarosewich 1990). Recognizable chondrules in NWA 428 range from 150–1800 μm in apparent diameter; the mean apparent diameter is 500 ± 280 μm (n = 50), identical to the estimated mean chondrule diameter in L3 chondrites (~500 μm; Rubin 2000). These characteristics demonstrate that NWA 428 is an L-group chondrite.

Petrologic Type

Olivine, low-Ca pyroxene, and plagioclase are fairly uniform in composition ($Fa_{24.4 \pm 0.6}$ mol%, $Fs_{20.5 \pm 0.4}$ mol%, and $Ab_{84.2 \pm 0.4}$ mol%, respectively; Table 1) as expected for equilibrated (type-4–6) OC. The mean sizes of metallic Fe-Ni and troilite grains in OC increase with petrologic type. Those in NWA 428 are 150 ± 150 μm (n = 75) and 100 ± 170 μm (n = 75), respectively. These sizes marginally exceed the mean values of those in type-5 and -6 OC (120 μm and 75–80 μm, respectively; Table 2 in Rubin et al. [2001]). Porphyritic olivine, porphyritic olivine-pyroxene, barred olivine, radial pyroxene, and cryptocrystalline chondrules are visible in NWA 428 but are poorly defined; they are well integrated with the matrix, consistent with petrologic type-6. Type-6 is also indicated by the occurrence of some coarse (20–60 μm-size) plagioclase grains. (Plagioclase grains 50 μm in size are characteristic of type-6 chondrites; Van Schmus and Wood 1967.) Clearly, NWA 428 is a type-6 chondrite.

Most low-Ca pyroxene in NWA 428 is inferred to be orthorhombic on the basis of its parallel optical extinction, consistent with a type-5 or type-6 classification. However, some coarse (100–150 μm-size) low-Ca pyroxene grains in NWA 428 are monoclinic; they have inclined extinction and exhibit polysynthetic twinning. Such grains are normally restricted to type-3 and, to a lesser extent, type-4 chondrites.

Brecciated Structure

NWA 428 is a breccia. UCLA slab LC 1887 contains ~10 vol% light-colored angular clasts ranging from ~1 mm to 9 × 15 mm in size. The clasts, which form sharp boundaries with the darker colored material in the host meteorite, consist of highly recrystallized L6 material. Plagioclase grains in these clasts range up to 60 μm in size.

Three varieties of predominantly opaque, shocked clasts are present. These clasts also form sharp boundaries with the host. There are 4 examples of the first variety in thin section UCLA 1682: they range in size from 160 × 300 μm to 340 × 1580 μm and consist of ~5–10 vol% of 1–2 μm-wide troilite veinlets that form intersecting networks transecting the silicate that makes up the bulk of the clasts. A few 4–30 μm-size isolated metal grains are also present.

One example of a second variety of shocked clast is related to the first. This 40 × 80 μm clast consists of ~30 vol% massive troilite and ~2 vol% metallic Fe-Ni enclosing 2–20 μm-size angular silicate grains.

One example of the third variety of shocked clast occurs in UCLA 1682. It is a 150 × 350 μm-size fragment of

Table 1. Compositions (wt%) of silicate and oxide phases in NWA 428.

	Olivine	Low-Ca pyroxene	Plagioclase	Chromite
Number of grains	10	17	4	5
SiO_2	38.1	55.0	64.4	<0.04
TiO_2	0.04	0.20	0.05	3.2
Al_2O_3	<0.04	0.22	20.6	5.9
Cr_2O_3	0.10	0.23	<0.04	56.2
FeO	22.7	13.7	0.59	30.4
MnO	0.45	0.46	<0.04	0.70
MgO	39.4	29.2	<0.04	3.1
CaO	0.05	0.89	2.2	<0.04
Na_2O	<0.04	<0.04	10.0	<0.04
K_2O	<0.04	<0.04	1.0	<0.04
Total	100.8	99.9	98.8	99.5
End member	$Fa_{24.4 \pm 0.6}$	$Fs_{20.5 \pm 0.4}Wo_{1.7 \pm 0.8}$	$Ab_{84.2 \pm 0.4}Or_{5.5 \pm 0.4}$	–

Table 2. Modal abundances of major phases in NWA 428.

	Vol%	Wt%[a]	Mean L (wt%)[b]
Silicate	91.6	85.8	85.0
Troilite	4.7	6.2	6.1
Metallic Fe-Ni	3.2	7.3	7.5
Chromite	0.27	0.36	0.6
Ilmenite	0.03	0.04	0.2
Limonite	0.17	0.21	0.0
Total	100.0	99.9	100.0
Number of points	2924	2924	–
Area (mm^2)	150	150	–

[a]Volume percent was converted into wt% using the following specific gravities: silicate 3.3; troilite 4.67; metallic Fe-Ni 7.95; chromite 4.7; ilmenite 4.72; and limonite 4.28.

[b]The normative mineralogy of L chondrites is from Table 4.1 in Dodd (1981). The total also includes 0.6 wt% apatite.

solidified silicate melt containing an elongated patch of rapidly solidified intergrowths of metal and troilite. The patch encloses 2–20 μm-size angular silicate grains and grain fragments. Numerous 1–8 μm-size spheroidal blebs of rapidly solidified metal-troilite are also present in the clast. The spheroidal shape of these opaque blebs indicate that they formed from melt droplets that were immiscible in the surrounding predominantly silicate melt.

Rare olivine grains in the shocked clasts are observable microscopically in transmitted light. Because individual olivine grains are thinner than the 30 μm section, discerning if the grains exhibit undulose extinction is difficult. However, the olivine grains do not appear to contain the planar fractures that are characteristic of shock stage S3.

Shock Features

Moderate silicate darkening is evident in some portions of NWA 428. This is caused by the dispersion within and around some silicate grains of small blebs of metallic Fe-Ni and troilite (e.g., Rubin 1992). The blebs most likely formed during shock heating when local temperatures in the rock exceeded that of the Fe-FeS eutectic (988°C). Silicate darkening occurs in rocks shocked to stage S3–S6 (Rubin 1992).

Several grains of polycrystalline troilite occur (Fig. 1a). Each of these assemblages contains 1 or more patches of troilite (4–60 μm in size) with different crystallographic orientations than the main troilite grain. Shock recovery experiments indicate that troilite becomes polycrystalline at shock pressures of 35 to 60 GPa (Schmitt et al. 1993), corresponding to shock stage S5–S6 (Stöffler et al. 1991).

A few large troilite nodules, ranging in size from 0.3 × 0.8 mm to 1.2 × 1.7 mm, occur in thin section UCLA 1682. Such nodules occur in many shocked chondrites (Rubin 1985) and are characteristic of shock stage S4–S6 (Rubin 1999).

Metallic Cu grains in NWA 428 occur among small irregularly shaped troilite grains within metallic Fe-Ni at troilite-metal boundaries (Fig. 1b). Rubin (1994) defined a petrographic parameter called occurrence abundance (OA) as 100 × ([number of occurrences]/mm^2) and found that OC with metallic Cu OA values ≥2.5 tend to have a higher mean shock stage than OC with values <2.5. Thirteen occurrences of metallic Cu patches (2–30 μm in size) occur in thin section UCLA 1682 (surface area = 150 mm^2), yielding an OA value of 8.7. This value is higher than 90% of the metallic Cu-bearing OC studied by Rubin (1994) and is consistent with a moderately high degree of shock. Metallic Cu probably forms when a rock is shocked to stage S3–S6 and metal-sulfide assemblages are melted. Upon cooling of this melt, taenite is

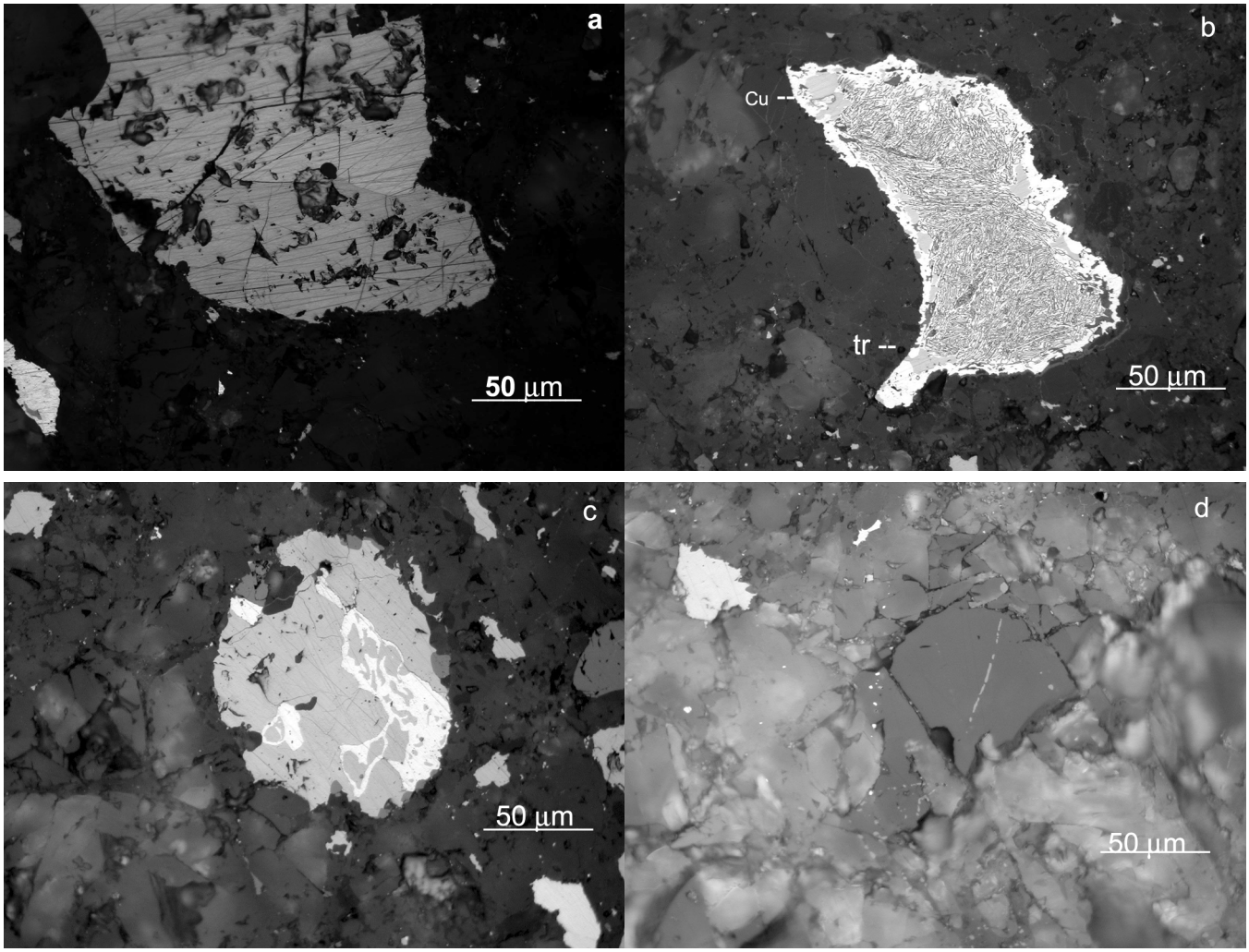

Fig. 1. Shock features involving opaque phases in NWA 428: a) polycrystalline troilite. This initially monocrystalline troilite grain has been broken into separate crystals. The crystal at the bottom is darker than the one at the upper right. Reflected light using the analyzer; b) nital-etched plessite grain consisting of μm-size intergrowths of kamacite and taenite. The plessite is surrounded by a thin rind of taenite (white). Near the edge of the grain are small patches of troilite (tr; medium gray) and one grain of metallic Cu (light gray with dark gray rim at upper left). Reflected light; c) small irregularly shaped troilite grains (medium gray) inside a metallic Fe-Ni (white) patch that is itself partially enclosed in massive troilite. Reflected light; d) small curvilinear chromite veinlet (light gray; center) inside an olivine grain fragment (dark gray). Reflected light.

the first phase to crystallize; because the solid-liquid distribution coefficient of Cu is less than 1, Cu is concentrated in the increasingly S-rich residual liquid. Eventually, Cu becomes supersaturated and precipitates at high-surface-energy sites such as metal-sulfide boundaries.

Irregularly shaped grains of troilite within metallic Fe-Ni (with or without the occurrence of metallic Cu) also indicate shock stage S3–S6 (Rubin 1994). These features formed by localized melting of metal-troilite assemblages, crystallization of taenite, and subsequent crystallization of small sulfide grains from the residual S-rich melt. NWA 428 possesses many such assemblages (Fig. 1c); they consist typically of 2–20 μm-size troilite grains within coarser (100–300 μm-size) metal grains.

The NWA 428 host (i.e., the region outside recognizable clasts) contains several 200–2000 μm-long metal-troilite veins. Stöffler et al. (1991) found that such veins occur in shock stage S3–S6 chondrites.

Duplex plessite (e.g., Buchwald 1975), consisting of intimate intergrowths of ~1 μm-long kamacite and taenite grains, occurs in some metal assemblages as 60–150 μm-wide patches rimmed by 1–4 μm-thick rinds of taenite (Fig. 1b). In some metal assemblages, kamacite occurs adjacent to the duplex plessite. The bulk duplex plessite grains have "M-shaped" Ni profiles with high Ni in the taenite rim and lower Ni in the plessitic interior. This compositional distribution of Ni results from solid-state diffusion and appears to have been produced by martensite decomposition (Massalski et al. 1966). Thus, the plessite likely formed from martensite that was annealed; the martensite itself formed from kamacite-taenite intergrowths that experienced localized shock melting and quenching. Martensite is most common in shock stage

S4–S6 chondrites (e.g., Taylor and Heymann 1970; Smith and Goldstein 1977).

NWA 428 also contains several chromite-plagioclase assemblages averaging ~150 μm in size. The assemblages are fine-grained, consisting of 0.5–4 μm-size irregular and rounded chromite grains (~30 vol%) surrounded by plagioclase or plagioclase-composition glass (~70 vol%). The plagioclase in the assemblages has a low impedance to shock compression and can melt during sufficiently intense impact events (corresponding to shock stage S3–S6). Heat from the molten plagioclase melts adjacent chromite grains. Rapid cooling of the melt produces the chromite-plagioclase assemblages (Rubin 2003).

Chromite veinlets occur in some mafic silicate grains (Fig. 1d). The veinlets are ~0.5 μm wide and up to 25 μm long; they consist of strings of 0.5–2 μm-size blebs and 2–10 μm-long needles of chromite. Veinlet formation is a byproduct of the production of chromite-plagioclase assemblages: chromite crystallizes within silicate fractures and the residual plagioclase melt continues to flow. Veinlets with little or no plagioclase remain (Rubin 2003).

Low-Ca clinopyroxene is common in pyroxene-bearing chondrules in type-3 OC and occurs in many type-4 OC. However, this phase is absent in type-5 and -6 OC because low-Ca clinopyroxene transforms into orthopyroxene at ≥630°C (Boyd and England 1965; Grover 1972). This is appreciably lower than the equilibration temperatures of type-5 and -6 OC (700–750°C and 820–930°C, respectively; Dodd 1981; Olsen and Bunch 1984). Hornemann and Müller (1971) and Stöffler et al. (1991) found that clinopyroxene lamellae parallel to (100) form within orthopyroxene grains at shock pressures of ~5 GPa. Because NWA 428 does not contain type-3 clasts (which would be expected to have low-Ca-clinopyroxene-bearing chondrules), the low-Ca clinopyroxene in NWA 428 (Fig. 2) seems likely to have formed during shock.

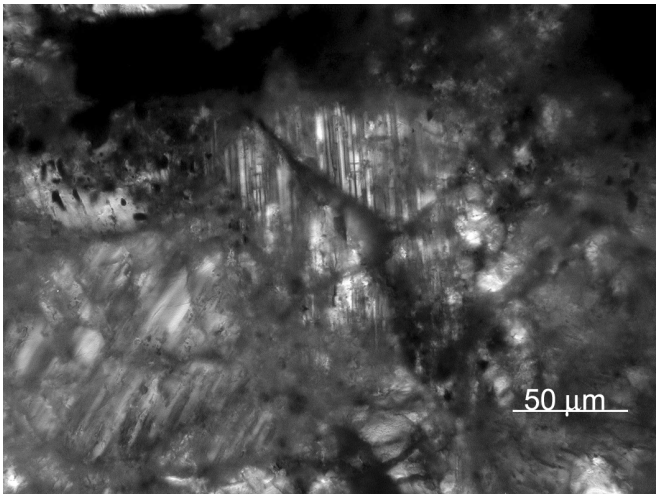

Fig. 2. Polysynthetically twinned low-Ca clinopyroxene grains. These grains were formed from shocked orthopyroxene. Transmitted light with crossed nicols and condenser lens.

Reliability of Petrographic Shock Indicators

To establish the case that the petrographic "shock-indicating" features in NWA 428 described above were indeed formed by shock processes, one must demonstrate that these features could not occasionally form in unshocked rocks. The reliability of these features as shock indicators rests on the observations that they occur most commonly in shocked OC and that silicate darkening, metal-sulfide veins, and metallic Cu are unlikely to have been produced through normal thermal metamorphic processes.

Stöffler et al. (1991) listed metal-sulfide veins as features characteristic of S3–S6 chondrites. Although metal-sulfide veins could conceivably form in a thermally metamorphosed OC if the temperature exceeded that of the Fe-FeS eutectic (988°C), Rubin (Forthcoming) identified such veins in only 26% (9/34) of the stage-S1, type-6 OC that he examined. That these 9 rocks were heated to higher-than-normal temperatures is unlikely because they do not appear to be any more recrystallized than other type-6 OC that lack metal-sulfide veins.

Rubin (1992) described major silicate darkening in several highly shocked chondrites including Stratford (L6, S4) and the Rose City (H5, S6) impact-melt breccia; both of these rocks also contain abundant metal-sulfide veins. That silicate darkening in NWA 428 was caused by thermal metamorphism seems unlikely. Although McSween et al. (1978) heated samples of LL3.1 Krymka to 900–1000°C for 1 week and found that troilite had melted and penetrated fractures in the silicate grains, Rubin (Forthcoming) found that less than half of the shock stage S1, petrologic type-6 OC that he examined exhibits silicate darkening. If silicate darkening were a normal consequence of thermal metamorphism, it should occur in virtually all type-6 OC.

Chromite veinlets and chromite-plagioclase assemblages constitute ~3 vol% of Jartai (L6, S4) and ~1 vol% of Hualapai Wash (L6, S4). They are present in the shock stage S6 impact-melt breccias Chico, Rose City, Smyer, and Yanzhuang; they also occur in several shock stage S5 chondrites, many S4 OC, and some S3 OC. The common occurrence of chromite veinlets and chromite-plagioclase assemblages in significantly shocked OC is consistent with their production during shock events (Rubin 2003).

Possibly, metallic Cu could form from melted metal-sulfide assemblages in OC that were heated above 988°C during thermal metamorphism. However, Rubin (1994) found that metallic Cu is no more abundant in type-6 OC than in type-4 OC, inconsistent with a high temperature metamorphic origin. Also, a significant positive correlation exists in OC between shock stage and the occurrence abundance of metallic Cu (Rubin 1994).

Because the petrographic shock indicators occur throughout the meteorite outside of the shocked clasts, NWA 428 clearly is not an unshocked rock that incorporated some highly shocked material during a brecciation event.

Ambiguities in Shock Stage Assignment

The petrologic characteristics of NWA 428 yield inconsistent shock stage assignments. Olivine grains throughout the meteorite exhibit sharp optical extinction and lack planar fractures and planar deformation features; they are characteristic of an unshocked (i.e., shock stage S1) rock. However, many other features of NWA 428 (silicate darkening, polycrystalline troilite, metallic Cu, large troilite nodules, irregularly shaped troilite grains within metallic Fe-Ni, metal and sulfide veins, plessite, chromite-plagioclase assemblages, chromite veinlets, and low-Ca clinopyroxene) indicate stage S3–S6. This range can be further constrained. Because polycrystalline troilite is characteristic of S4–S5 (Bennett and McSween 1996; Schmitt et al. 1993), a lower limit of S4 is indicated. This lower limit is consistent with the presence of metal-troilite veins, large troilite nodules, and duplex plessite (formed from annealed martensite). On the other hand, because no evidence exists of wide-spread silicate melt in NWA 428 (as expected in an impact-melt breccia of shock stage S6; Stöffler et al. 1991), an upper limit of S5 is indicated. Therefore, NWA 428 was once shocked to stage S4–S5.

The ambiguity in shock stage assignment could be resolved if the olivine was shocked along with the rest of NWA 428 and then the rock experienced post-shock annealing. Relatively rapid elemental diffusion in olivine could heal the shock-damaged olivine crystal lattice during annealing. Bauer (1979) demonstrated that shock-induced microfractures in olivine could be annealed in 20 min at 700–900°C. The data of Chakraborty (1997) for Fe-Mg interdiffusion rates in olivine at ~950°C show diffusion over approximately 6 μm within a year. Although the data of Chakraborty do not extend to lower temperatures, that olivine annealing could be accomplished at such temperatures (e.g., 600°C) in correspondingly longer time periods seems likely.

Annealing temperatures could not have exceeded 630°C or the low-Ca clinopyroxene in the rock would have been transformed into orthopyroxene. The absence of low-Ca clinopyroxene in type-5 and -6 OC suggests that post-metamorphic, post-shock annealing of NWA 428 (which contains low-Ca clinopyroxene) reached levels approximating that of the low end of petrologic type-4; Dodd (1981) estimated type-4 OC to have been heated to ~600–700°C.

Thermal and Shock History

NWA 428 underwent successive episodes of thermal metamorphism to type-6 levels, shock metamorphism to stage S4–S5, brecciation, and post-shock annealing to ~600°C.

During the initial episode of thermal metamorphism to petrologic type-6, mineral phases developed relatively uniform compositions, chondrules were texturally integrated into the matrix, chondrule glass devitrified, coarse plagioclase grains crystallized, metal and sulfide grains coarsened, and low-Ca clinopyroxene transformed into orthopyroxene.

During shock metamorphism to stage S4–S5 levels, olivine developed mosaic extinction, planar fractures, and planar deformation features; low-Ca clinopyroxene lamellae developed along (100) in orthopyroxene; and plagioclase and chromite were melted locally, producing chromite-plagioclase assemblages and chromite veinlets upon crystallization. Metal and sulfide were melted and mobilized, producing metal and sulfide veins, large troilite nodules, and irregular grains of troilite within metal (in some cases associated with metallic Cu). Metal and sulfide in some thin veins contracted into individual blebby droplets. In addition, some grains of troilite became polycrystalline, and some metal grains were melted and quenched to produce martensite.

Impacts produced post-shock brecciation. Some highly recrystallized clasts, shocked clasts, and shock-melted clasts were fragmented and dispersed throughout the parent body region from which the NWA 428 breccia formed. The low shock stage (S1) of the highly recrystallized clasts indicates that they were introduced into NWA 428 before annealing.

During post-shock annealing to low type-4 levels, low-Ca clinopyroxene would not have transformed into orthopyroxene, but olivine grains would have healed their damaged lattices and developed sharp optical extinction. Martensite would have unmixed to form plessite. Although fine-grained polycrystalline troilite could potentially be transformed into single crystals during moderate annealing, annealing to type-4 levels seems likely to allow moderately coarse-grained polycrystalline troilite to survive. Annealing to type-4 levels would probably fail to erase other shock-indicating features in NWA 428. Chromite veinlets, chromite-plagioclase assemblages, metal and sulfide blebs, metal and sulfide veins, large troilite nodules, and irregular grains of troilite in metallic Fe-Ni could coarsen slightly during annealing to type-4 levels but would still be recognizable. Metallic Cu is a very stable phase; once nucleated, it should survive annealing to metamorphic levels appreciably higher than type-4.

Petrologic Similarities to MIL 99301

As described by Rubin (2002), MIL 99301 (LL6) resembles NWA 428 (L6) in exhibiting silicate darkening and containing polycrystalline troilite, metallic Cu, irregularly shaped troilite grains within metallic Fe-Ni, plessite, chromite-plagioclase assemblages, chromite veinlets, and coarse grains of low-Ca clinopyroxene. These features indicate that MIL 99301 and NWA 928 experienced very similar thermal and shock histories. MIL 99301 also was metamorphosed to type-6 levels, shocked to stage S4–S5, and then annealed to a level approximating petrologic type-4.

Ar-Ar age data indicate that annealing in MIL 99301 took place ~4.26 Ga ago (Dixon et al. 2003). At this late date, ~300 Ma after accretion, impacts are the only plausible heat source; any ^{26}Al that may have been present when the asteroid accreted would have decayed away by that time. Although NWA 428 has not yet been analyzed by Ar-Ar techniques, its petrologic similarities to MIL 99301 strongly suggest that it was also annealed by an impact. Impact heating has, thus, affected both the L and the LL parent asteroids.

Some shock stage S1 H6 chondrites also contain relict shock features. For example, Frontier Mountains (FRO) 90088 exhibits silicate darkening and contains chromite veinlets, chromite-plagioclase assemblages, irregular grains of troilite within metallic Fe-Ni, rapidly solidified metal-sulfide intergrowths, metal and sulfide veins, a large silicate melt vein, and silicate-rich melt pockets (Rubin Forthcoming). These features indicate that FRO 90088 experienced a thermal and shock history similar to that of NWA 428 and MIL 99301. If the silicate melt vein in FRO 90088 had formed before metamorphism to petrologic type-6, it would probably have been texturally integrated with the matrix and rendered virtually unrecognizable. Hence, the vein most likely formed after the initial epoch of thermal metamorphism. Similarly, if the rapidly solidified metal-sulfide intergrowths in FRO 90088 antedated thermal metamorphism, they also would probably have been obliterated. Thus, these features were formed after thermal metamorphism; their preservation indicates that post-shock annealing was mild.

Post-shock annealing is most readily accomplished by deposition of shocked rocks among debris at the floor of an impact crater or in a hot ejecta blanket outside the crater. The same impact responsible for the shock features in these rocks can provide the heat necessary for annealing. This is particularly the case for porous asteroids where collisional kinetic energy is distributed through relatively small volumes of material and efficiently converted into heat in the crater vicinity (Melosh 1989; Housen and Holsapple 1999). Because many asteroids appear to be low density, high porosity rubble piles (e.g., Veverka et al. 1999; Cheng and Barnouin-Jha 1999; Bottke et al. 1999), one can conclude that cratering events were commonly responsible for episodes of shock and post-shock annealing.

The existence of type-6 H, L, and LL chondrites that have experienced successive episodes of thermal metamorphism, shock metamorphism, and post-shock annealing demonstrates that this sequence of processes occurred on the 3 principal OC parent asteroids.

Acknowledgments–I thank T. J. McCoy and T. G. Sharp for helpful reviews. This work was supported mainly by NASA Grant No. NAG5–12967 (A. E. Rubin).

Editorial Handling—Dr. Randy Korotev

REFERENCES

Akridge G., Benoit P. H., and Sears D. W. G. 1998. Regolith and megaregolith formation of H chondrites: Thermal constraints on the parent body. *Icarus* 132:185–195.

Bauer J. F. 1979. Experimental shock metamorphism of mono- and polycrystalline olivine: A comparative study. Proceedings, 10th Lunar and Planetary Science Conference. pp. 2573–2596.

Bennett M. E. and McSween H. Y. 1996. Shock features in iron-nickel metal and troilite of L-group ordinary chondrites. *Earth and Planetary Science Letters* 31:255–264.

Bottke W. F., Richardson D. C., Michel P., and Love S. G. 1999. 1620 Geographos and 433 Eros: Shaped by planetary tides. *The Astronomical Journal* 117:1921–1928.

Boyd F. R. and England J. L. 1965. The rhombic enstatite-clinoenstatite inversion. *Annual report of the Director, Geophysical laboratory.* Washington D.C.: Carnegie Institution on Washington. pp. 117–120.

Brearley A. J. and Jones R. H. 1998. Chondritic meteorites. In *Planetary materials,* edited by Papike J. J. Washington D.C.: Mineralogical Society of America. pp. 3-1–3-398.

Buchwald V. F. 1975. *Handbook of iron meteorites.* Berkeley: University of California Press.

Chakraborty S. 1997. Rates and mechanisms of Fe-Mg interdiffusion in olivine at 980–1300°C. *Journal of Geophysical Research* 102: 12317–12331.

Cheng A. F. and Barnouin-Jha O. S. 1999. Giant craters on Mathilde. *Icarus* 140:34–48.

Dixon E. T., Bogard D. D., and Rubin A. E. 2003. ^{39}Ar-^{40}Ar evidence for an ~4.26 Ga impact heating event on the LL parent body (abstract #1108). 34th Lunar and Planetary Science Conference.

Dodd R. T. 1981. *Meteorites—A petrologic-chemical synthesis.* Cambridge: Cambridge University Press. 368 p.

Gomes C. B. and Keil K. 1980. *Brazilian stone meteorites.* Albuquerque: University of New Mexico Press.

Grimm R. E. and McSween H. Y. 1989. Water and the thermal evolution of carbonaceous chondrite parent bodies. *Icarus* 82: 244–280.

Grimm R. E. and McSween H. Y. 1993. Heliocentric zoning of the asteroid belt by aluminum-26 heating. *Science* 259:653–655.

Grover J. E. 1972. The stability of low-clinoenstatite in the system $Mg_2Si_2O_6$-$CaMgSi_2O_6$ (abstract). *Transactions of the American Geophysical Union* 53:539.

Herndon J. M. and Herndon M. A. 1977. Aluminum-26 as a planetoid heat source in the early solar system. *Meteoritics* 12:459–465.

Hornemann U. and Müller W. F. 1971. Shock-induced deformation twins in clinopyroxene. *Neues Jahrbuch für Mineralogie* 6:247–256.

Housen K. R. and Holsapple K. A. 1999. Impact cratering on porous low-density bodies (abstract #1228). 30th Lunar and Planetary Science Conference.

Jarosewich E. 1990. Chemical analyses of meteorites: A compilation of stony and iron meteorite analyses. *Meteoritics* 25:323–337.

Keil K. 2000. Thermal alteration of asteroids: Evidence from meteorites. *Planetary and Space Science* 48:887–903.

Massalski T. B., Park F. R., and Vassamillet L. F. 1966. Speculations about plessite. *Geochimica et Cosmochimica Acta* 30:649–662.

McSween H. Y., Taylor L. A., and Lipschutz M. E. 1978. Metamorphic effects in experimentally heated Krymka L3. chondrite. Proceedings, 9th Lunar and Planetary Science Conference. pp. 1437–1447.

McSween H. Y., Ghosh A., Grimm R. E., Wilson L., and Young E. D. 2002. Thermal evolution models of asteroids. In *Asteroids III,* edited by Bottke W. F., Cellino A., Paolicchi P., and Binzel R. P. Tucson: University of Arizona Press. pp. 559–571.

Melosh H. J. 1989. *Impact cratering: A geologic process*. New York: Oxford University Press.

Olsen E. J. and Bunch T. E. 1984. Equilibration temperatures of the ordinary chondrites: A new evaluation. *Geochimica et Cosmochimica Acta* 48:1363–1365.

Reeves H. and Audouze J. 1968. Early heat generation in meteorites. *Earth and Planetary Science Letters* 4:135–141.

Rubin A. E. 1983a. Impact melt-rock clasts in the Hvittis enstatite chondrite breccia: Implications for a genetic relationship between EL chondrites and aubrites. Proceedings, 14th Lunar and Planetary Science Conference. pp. B293–B300.

Rubin A. E. 1983b. The Atlanta enstatite chondrite breccia. *Meteoritics* 18:113–121.

Rubin A. E. 1984. The Blithfield meteorite and the origin of sulfide-rich, metal-poor clasts and inclusions in brecciated enstatite chondrites. *Earth and Planetary Science Letters* 67: 273–283.

Rubin A. E. 1985. Impact melt products of chondritic material. *Reviews of Geophysics* 23:277–300.

Rubin A. E. 1990. Kamacite and olivine in ordinary chondrites: Intergroup and intragroup relationships. *Geochimica et Cosmochimica Acta* 54:1217–1232.

Rubin A. E. 1992. A shock-metamorphic model for silicate darkening and compositionally variable plagioclase in CK and ordinary chondrites. *Geochimica et Cosmochimica Acta* 56: 1705–1714.

Rubin A. E. 1994. Metallic copper in ordinary chondrites. *Meteoritics* 29:93–98.

Rubin A. E. 1999. Formation of large metal nodules in ordinary chondrites. *Journal of Geophysical Research—Planets* 104: 30799–30804.

Rubin A. E. 2000. Petrologic, geochemical, and experimental constraints on models of chondrule formation. *Earth Science Reviews* 50:3–27.

Rubin A. E. 2002. Post-shock annealing of Miller Range 99301: Implications for impact heating of ordinary chondrites. *Geochimica et Cosmochimica Acta* 66:3327–3337.

Rubin A. E. 2003. Chromite-plagioclase assemblages as a new shock indicator: Implications for the shock and thermal histories of ordinary chondrites. *Geochimica et Cosmochimica Acta* 67: 2695–2709.

Rubin A. E. Forthcoming. Post-shock annealing and post-annealing shock in equilibrated ordinary chondrites: Implications for the thermal and shock histories of chondritic asteroids. *Geochimica et Cosmochimica Acta.*

Rubin A. E., Scott E. R. D., and Keil K. 1997. Shock metamorphism of enstatite chondrites. *Geochimica et Cosmochimica Acta* 61: 847–858.

Rubin A. E., Ulff-Møller F., Wasson J. T., and Carlson W. D. 2001. The Portales Valley meteorite breccia: Evidence for impact-induced melting and metamorphism of an ordinary chondrite. *Geochimica et Cosmochimica Acta* 65:323–342.

Russell S. S., Zipfel J., Folco L., Jones R., Grady M. M., McCoy T., and Grossman J. N. 2003. The Meteoritical Bulletin, No. 87. *Meteoritics & Planetary Science* 38:A189–A248.

Schmitt R. T., Deutsch A., and Stöffler D. 1993. Shock effects in experimentally shocked samples of the H6 chondrite Kernouvé abstract. *Meteoritics* 28:431–432.

Smith B. A. and Goldstein J. I. 1977. The metallic microstructures and thermal histories of severely reheated chondrites. *Geochimica et Cosmochimica Acta* 41:1061–1072.

Stöffler D., Keil K., and Scott E. R. D. 1991. Shock metamorphism of ordinary chondrites. *Geochimica et Cosmochimica Acta* 55: 3845–3867.

Taylor G. J. and Heymann D. 1970. Electron microprobe study of metal particles in the Kingfisher meteorite. *Geochimica et Cosmochimica Acta* 34:677–687.

Urey H. C. 1955. The cosmic abundances of potassium, uranium, and thorium and the heat balances of the Earth, the Moon, and Mars. *Proceedings of the National Academy of Science* 41:127–144.

Van Schmus W. R. and Ribbe P. H. 1968. The composition and structural state of feldspar from chondritic meteorites. *Geochimica et Cosmochimica Acta* 32:1327–1342.

Van Schmus W. R. and Wood J. A. 1967. A chemical-petrologic classification for the chondritic meteorites. *Geochimica et Cosmochimica Acta* 31:747–765.

Veverka J., Thomas P., Harch A., Clark B., Bell J. F., III, Carcich B., Joseph J., Murchie S., Izenberg N., Chapman C., Merline W., Malin M., McFadden L., and Robinson M. 1999. NEAR encounter with asteroid 253 Mathilde: Overview. *Icarus* 140:3–16.

Wilson L., Keil K., Browning L. B., Krot A. N., and Bourcier W. 1999. Early aqueous alteration, explosive disruption, and reprocessing of asteroids. *Meteoritics & Planetary Science* 34: 541–557.

Wlotzka F. 1993. A weathering scale for the ordinary chondrites abstract. *Meteoritics* 28:460.